Journal of Inorganic Biochemistry 236 (2022) 111945

Contents lists available at ScienceDirect

Journal of Inorganic Biochemistry

journal homepage: www.elsevier.com/locate/jinorgbio

# $Cu^{2+}$ ions modulate the interaction between α-synuclein and lipid membranes

Hongzhi Wang [a], Cecilia Mörman [a,b], Rebecca Sternke-Hoffmann [a], Chia-Ying Huang [c], Andrea Prota [a], Pikyee Ma [a], Jinghui Luo [a,*]

[a] Department of Biology and Chemistry, Paul Scherrer Institute, 5232 Villigen, Switzerland
[b] Department of Biosciences and Nutrition, Karolinska Institutet, 141 52 Huddinge, Sweden
[c] Swiss Light Source at Paul Scherrer Institut, Forschungstrasse 111, Villigen-PSI, Villigen 5232, Switzerland

ARTICLE INFO

*Keywords:*
α-Synuclein
$Cu^{2+}$ ions
LCP
SAXS
*In-cell* NMR
Parkinson's disease

ABSTRACT

α-synuclein protein aggregates are the major constituent of Lewy bodies, which is a main pathogenic hallmark of Parkinson's disease. Both lipid membranes and $Cu^{2+}$ ions can bind to α-synuclein and modulate its aggregation propensity and toxicity. However, the synergistic effect of copper ions and lipid membranes on α-synuclein remains to be explored. Here, we investigate how $Cu^{2+}$ and α-synuclein simultaneously influence the lipidic structure of lipidic cubic phase(LCP) matrix by using small-angle X-ray scattering. α-Syn proteins destabilize the cubic-Pn3m phase of LCP that can be further recovered after the addition of $Cu^{2}$ ions even at a low stoichiometric ratio. By using circular dichroism and nuclear magnetic resonance, we also study how lipid membranes and $Cu^{2+}$ ions impact the secondary structures of α-synuclein at an atomic level. Although the secondary structure of α-synuclein with lipid membranes is not significantly changed to a large extent in the presence of $Cu^{2+}$ ions, lipid membranes promote the interaction between α-synuclein C-terminus and $Cu^{2+}$ ions. The modulation of $Cu^{2+}$ ions and lipid membranes on α-synuclein dynamics and structure may play an important role in the molecular pathogenesis of Parkinson's disease.

## 1. Introduction

α-synuclein (α-Syn), an intrinsically unfolded protein, is involved in neurotransmitter release from the presynaptic terminal, and is also a causative agent of Parkinson's disease (PD). α-Syn comprises three important domains: the N-terminal, the non-amyloid-component (NAC), and the C-terminal domains. Upon binding to lipid vesicles, the N-terminal and NAC domains of α-Syn undergo the structural transition from random coil to α-helix secondary structures [1]. As shown in Fig. 1, the N-terminal helical domain functions as the membrane anchor, while the NAC domain acts as a sensor for lipids and is the determinant for the binding affinity between α-Syn and lipid membranes. The disordered C-terminal region only displays weak association with lipid membranes [2]. Lipid membranes play a crucial role in the binding, internalization, aggregation, and toxicity of α-Syn, and vice versa [1,3]. For instance, α-Syn changes membrane curvature [4], membrane remodeling [5], the chain order, and the thermotropic phase behavior of anionic lipid vesicles [6] as well as membrane expansion [7]. Like $Zn^{2+}$ ions, $Cu^{2+}$ ions levels in Alzheimer's disease (AD) and Parkinson's disease (PD) brains substantially vary from those in the healthy brain, although the exact concentrations remain to be precisely determined in Table 1. In neurodegenerative diseases, $Cu^{2+}$ ions presumably play important roles in the interaction between lipid membranes and amyloid proteins [8,9]. In addition, $Cu^{2+}$ ions can catalyze protein oxidation, leading to subsequent denaturation [10]. Overall, both $Cu^{2+}$ ions and lipid membranes play essential roles in the physiology and pathology of PD. The synergistic effect of $Cu^{2+}$ ions and lipid membranes on α-Syn dynamics and structure remains to be explored for further understanding of the

*Abbreviations:* α-synuclein, α-Syn; Parkinson's disease, PD; Alzheimer's disease, AD; Lipidic cubic phase, LCP; Circular dichroism, CD; Nuclear magnetic resonance, NMR; Small-angle X-ray scattering, SAXS; Amino acid, aa; Cerebrospinal fluid, CSF; Substantia nigra, SN; Hippocampus, HP; Cerebellum, CB; Monoolein, MO; Phosphatidylcholine, PC; Phosphatidylserine, PS; 1-palmitoyl-2-oleoyl-sn-glycero-3-phospho-L-serine, POPS; 1,2-dioleoyl-sn-glycero-3-phosphoglycerol, DOPG; Isopropyl β-d-thiogalactopyranoside, IPTG; Ion exchange chromatography, IEX; Size exclusion chromatography, SEC; In meso in situ serial crystallography, IMISX; Cyclic olefin copolymer, COC.

* Corresponding author.
*E-mail address:* Jinghui.luo@psi.ch (J. Luo).

https://doi.org/10.1016/j.jinorgbio.2022.111945
Received 8 April 2022; Received in revised form 20 July 2022; Accepted 22 July 2022
Available online 28 July 2022

molecular pathogenesis in PD.

Lipid vesicles, like small unilamellar vesicles and large unilamellar vesicles, have been used for studying α-Syn. Such systems are typically prepared in a high-salt buffer condition [7], and differ from the amphiphilic and air-tight conditions in the brain. In comparison to lipid vesicles, the lipidic cubic phase (LCP) matrix may provide a brain mimicking condition. LCP is usually in Pn3m and Ia3d phases and is often employed and embedded with membrane proteins used for crystallization [11,12]. The matrix forms a three-dimensional lipidic array with an appropriate proportion of lipid and water, and has a transparent bicontinuous bilayer by intercommunicating aqueous channels [11,12]. The lipid curvature of LCP can be adapted to the mixture with chemicals [13]. Likewise, α-Syn influences its lipid binding affinity by modulating the curvature of lipid membranes [14,15]. LCP may provide a brain mimicking condition for studying the interaction between protein and lipid membranes. Lipid phase changes of LCP upon protein binding may also enable to sense the lipid interaction with protein at mesoscopic scales. In parallel, the inner and outer lipid membranes of *E.coli* cells also provide a rather space-compact and air-tight environment for the interaction between lipids and protein [16]. Compared to lipid vesicles, *E.coli* cells and LCP can provide a unique and brain-mimicking environment for studying the interaction between lipid membranes and α-Syn in the presence of $Cu^{2+}$ ions.

Here, we firstly investigated the synergetic effect of $Cu^{2+}$ ions and α-Syn on the lipid bilayer structure of LCP at mesoscopic scales by using small-angle X-ray scattering (SAXS). Secondly, the influence of $Cu^{2+}$ ions on the secondary structure transition of α-Syn proteins in the presence of lipid membranes was studied using circular dichroism (CD). Finally, nuclear magnetic resonance (NMR) was further employed to investigate how $Cu^{2+}$ ions modulate α-Syn proteins at the atomic level both in buffer conditions and when α-Syn is expressed within the periplasm of *E.coli*. Briefly, our study reports the synergetic effect of $Cu^{2+}$ ions and different lipid membranes on α-Syn structure, and vice versa. These interactions at the atomic and mesoscopic levels in air-tight and amphiphilic environments mimicking the human brain state may broaden our understanding of the molecular mechanism of α-Syn in the pathogenesis of PD.

## 2. Results

### 2.1. $Cu^{2+}$ ions reverse the effect of α-Syn on the mesoscopic structure of LCP

Monoolein (MO) is a commonly used host lipid inLCP crystallization and produces a Pn3m cubic phase when mixed with water at a volume ratio of 3:2 at 20 °C. MO is not a natural component of cell membranes, however, it forms mimetic lipid bilayers which can be adapted by the addition of test lipids and chemicals. For crystallization of membrane proteins, natural lipids such as phosphatidylcholine (PC), phosphatidylserine (PS), and cholesterol are commonly added to the LCP system in order to achieve a more natural system to aid the crystallization of the target protein [12,30]. PS is the major acidic phospholipids localized exclusively in the cytoplasmic leaflet in neural tissues, where it participates in forming protein docking sites that are crucial for the activation of signal pathways involved in neuronal survival, neurite growth, and synaptogenesis [31]. In addition, PS is a lipid composition of synaptic vesicles that are responsible for the storage and exocytosis of neurotransmitters upon the arrival of an action potential [32] and related to PD [33]. Besides, α-Syn selectively interacts with anionic lipids like PS [34]. Therefore, to obtain a more physiologically relevant membrane, we prepared the lipidic matrix with 1-palmitoyl-2-oleoyl-sn-glycero-3-phospho-L-serine (POPS) and MO at molar ratios of 1%, 5%, and 10%, respectively, which were characterized by SAXS. In Fig. 2A-D, In the presence of MO with 1% or 5% POPS, the space group of the lipidic cubic phase remained as Pn3m with bicontinuous inverse cubic structures. The phase changed after the supplement of 10% POPS into MO. Therefore, the lipidic matrix with MO and 5% POPS was selected as a physiologically relevant model to investigate the interaction between α-Syn and LCP. As shown in Fig. 2E, α-Syn at a final concentration of 34 μM changed the Pn3m phase of MO + 5% POPS in 20 mM Tris-HCl buffer, pH 7.2. It suggests that α-Syn destabilizes the lipidic cubic system under the experimental conditions.

To study whether $Cu^{2+}$ ions influence the effect of α-Syn on the lipidic phase at mesoscopic scales, we prepared the MO lipidic matrix with 5% POPS in the presence of 34 μM α-Syn with 17 or 83 μM $Cu^{2+}$ ions. The addition of $Cu^{2+}$ ions converted the phase back to the Pn3m phase compared to that with α-Syn alone in Fig. 2F-G. As a control, $Cu^{2+}$ ions alone did not considerably change the phase of LCP shown in Fig. S1. Taken together, $Cu^{2+}$ ions counteracted the detrimental effect of α-Syn on the lipid structure of LCP (similar results were obtained in the presence of zinc, as shown in Fig.S2).

### 2.2. $Cu^{2+}$ ions modulate the effect of liposomes on the secondary structure transition of α-Syn

1,2-dioleoyl-sn-glycero-3-phosphoglycerol (DOPG) is another negatively charged phospholipid suitable for liposome preparation. In comparison to the lipidic mesoscopic studies by SAXS, we used lipid vesicles with different lipid curvatures to investigate how copper ions and DOPG liposomes influence the secondary structure of α-Syn by CD

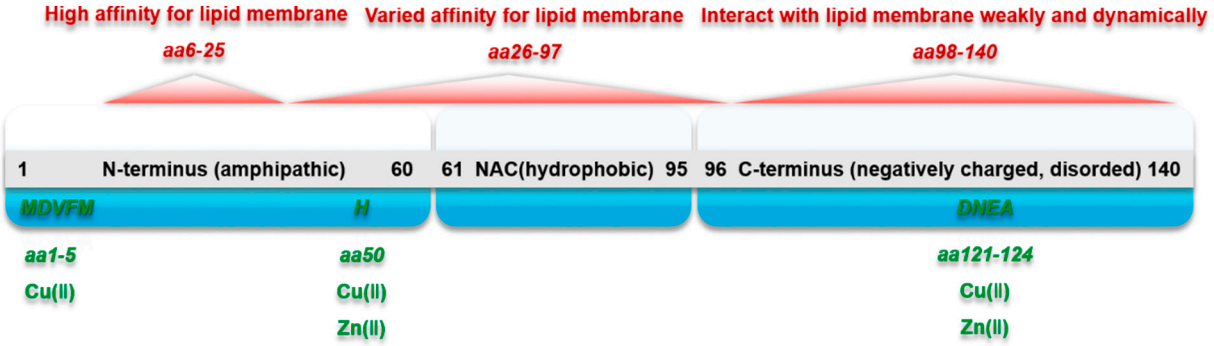


**Fig. 1.** Interactions of α-Syn with lipid membranes. α-Syn consists of three domains including the N-terminal domain (aa 1–60), the NAC domain (aa 61–95), and the C-terminal domain (aa 96–140) [1]. The N-terminal and NAC regions (amino acid residues 1–95) of a-synuclein contain seven 11-amino acid imperfect repeats with a highly conserved hexamer motif (KTKEGV). Most of the N-terminal part of α-Syn forms an α-helical structure upon binding to lipid membranes with a high affinity (aa 6-25), while the central part (aa 26-97) interacts with lipid membranes with a variable affinity depending on the lipid composition [1]. The C-terminus (aa 98-140) only interacts weakly with lipid membranes weakly and dynamically [1]. $Cu^{2+}$ ions and $Zn^{2+}$ ions have specific binding regions on α-Syn (amino acids highlighted in green) [8,17–19].

spectroscopy. The effect of $Cu^{2+}$ ions on the secondary structure transition of α-Syn was investigated by titrating $Cu^{2+}$ ions into the α-Syn solution to final concentrations of 0, 5, 25, 75, 150 and 300 μM. The signal of the random coil structure of α-Syn gradually disappeared as the concentration of $Cu^{2+}$ ions increased (data not shown here). Later, we also investigated the influence of DOPG liposomes on the secondary structure of α-Syn by titrating the liposomes with or without 300 μM $Cu^{2+}$ ions. The CD spectra from 190 to 260 nm at 37 °C were recorded immediately after each titration step of DOPG to quantify the secondary structure of α-Syn. It shows in Fig. 3A and B (data with standard deviations are shown in Fig.S4) that the CD spectra of α-Syn alone displayed a characteristic minimum at ~198 nm, corresponding to the random coil structure of an intrinsically disordered protein. α-Syn gradually converts to a typical α-helical structure as DOPG liposomes are titrated in the absence and presence of $Cu^{2+}$ ions, as indicated by the characteristic minima at 208 nm and 222 nm and a peak at 193 nm (Fig. 3). At a low ratio of DOPG to $Cu^{2+}$ ions, α-Syn remained the similar α-helical structure as observed in the absence of $Cu^{2+}$ ions (Fig. 3C). The α-helical signal of α-Syn slightly increased as the ratio of DOPG to $Cu^{2+}$ ions increased above 1:3. A similar behavior has been observed in the presence of $Zn^{2+}$ in Fig. S3. Our CD data agree with the previous studies that α-Syn is an intrinsically disordered protein and binds to the surface of lipid membranes, followed by a transition to α-helical structures in the N-terminus and/or NAC domain and induction of the aggregation of α-Syn [1]. The presence of $Cu^{2+}$ ions slightly changed the structure of α-Syn at a concentration of lipid vesicles above 100 μM. This may be explained by that α-Syn interacts with lipid membranes with high affinity towards the N-terminus and that $Cu^{2+}$ ions can slightly induce the helical structure formation of the N-terminus or NAC domain of α-Syn in the presence of DOPG. It seems that $Cu^{2+}$ ions do not alter the membrane-bound α-Syn conformation at a lipid/$Cu^{2+}$ ratio of 20:1 [35]. In our study, we used a much lower lipid/$Cu^{2+}$ ratio which might explain the discrepancy of the results from the previous study. Taken together, the results from the CD experiments indicate that $Cu^{2+}$ ions slightly enhanced the effect of the liposomes on the secondary structure transition of α-Syn proteins only above a lipid/Cu ratio of 1:3.

### 2.3. $Cu^{2+}$ ions interact with α-Syn in both buffer solution and E.coli cells

In order to investigate the effect of $Cu^{2+}$ ions on α-Syn in a lipidic environment, we took in-cell NMR measurements of α-Syn expressed in the periplasm of *E.coli* [16] where α-Syn proteins spontaneously interact with cellular membranes (Fig. 4). To estimate the concentration of α-Syn in the *E.coli* cells, we compared the amide cross-peak intensities in the heteronuclear single quantum correlation ($^1H$–$^{15}N$-HSQC)spectra of α-Syn in the cells to the intensities of a known 100 μM concentration of α-Syn in buffer conditions (Fig. 4A). The corresponding α-Syn concentration in the cells was determined to be approximately 60% of the one in buffer, corresponding to a theoretical α-Syn concentration of 60 μM. Noteworthy, under buffer conditions α-Syn is mainly unstructured, but in cellular conditions, some of the cross-peaks show different chemical shifts which are indicative of a change in structure (Fig. 4A). Especially residues of L8, T44, and V48 exhibit significant chemical shift changes (Δδ), highlighted in Fig. 4A.

To confirm the $Cu^{2+}$ ion interaction in a simple model system, $^1H$–$^{15}N$-HSQC spectra of 100 μM $^{15}N$-α-Syn in 20 mM potassium phosphate buffer pH 7.4 with 150 mM NaCl in the absence and presence of 1 mM $Cu^{2+}$ ions were recorded (Fig. 4B). The amide crosspeak signal intensities were overall reduced by 40–60%, and an especially significant reduction around residue H50 was observed. Histidine is a well-known metal ion interacting residue, and H50, as well as Met located at the first amino acid position of α-Syn (Met 1) are typically important for the $Cu^{2+}$ ion coordination [35–37]. Small chemical shift changes were also detected. Line broadening of the signals due to paramagnetic effects of the $Cu^{2+}$ ions likely explains the detected changes in the HSQC spectra in the presence of $Cu^{2+}$ ions, together with the chemical exchange. Hence the resonance signals for the residues directly involved or close to the $Cu^{2+}$ interaction are reduced in signal intensity. We also used a more complex model system to study the $Cu^{2+}$ interaction in *E.coli* cells. *E.coli* cells with a theoretical α-Syn concentration of 60 μM were incubated with an increased concentration of $Cu^{2+}$ ions (5 mM) administered to the extracellular environment of the cells, since only a proportion of $Cu^{2+}$ ions applied extracellularly can translocate into the periplasm of *E. coli* cells (Fig. 4C). The copper ions may remain as $Cu^{2+}$ rather than $Cu^{+}$, due to lack of sufficient NADH dehydrogenase-2 (Ndh-2, a cupric reductase) in inner membranes for the conversion of $Cu^{2+}$ into $Cu^{+}$, and also because of the oxidizing environment in the periplasm [38]. It is very difficult to precisely measure the concentration of $Cu^{2+}$ in the periplasm, the ions probably traverse the outer membrane through porins, like outer membrane protein C (OmpC) and outer membrane protein F (OmpF) [38]. The final copper concentration in the periplasm for living *E.coli* was estimated at 750 μM to maintain the homeostasis through porins [39,40], even though the solution concentration of $Cu^{2+}$ outside the *E.coli* cells during the experiment is much higher. Overall, the effect of $Cu^{2+}$ ions on α-Syn was similar to that of the $Cu^{2+}$-effect on α-Syn in buffer conditions. Despite that a more pronounced C-terminal interaction effect (involving residues A124-A140) in *E.coli* cells was observed compared to in buffer conditions, this indicates that $Cu^{2+}$ ions are readily transported across the outer cell membrane and interacted with the periplasmic α-Syn proteins under the test conditions. It has been previously reported that only the N-terminal domain of α-Syn interacts and converts into a α-helical conformation in the presence of lipid vesicles or detergent micelles [55]. The C-terminal domain remains free and unfolded and does not exhibit any interaction with lipid vesicles. These suggest that $Cu^{2+}$ promotes the interaction between the C-terminal domain of α-Syn and lipid membranes.

## 3. Discussion

α-Syn proteins possess various conformations under different conditions [41–43]. For instance, the partially α-helical structure in the membrane-bound state [2], is essentially important for both the physiological functions and pathological roles of α-Syn [44]. Metal ions like $Cu^{2+}$ act as a crucial player both for the properties of lipid membranes

**Table 1**
Variation of copper ions and zinc ions in Alzheimer's and Parkinson's disease patients.

| Location | Cu | | | Zn | | |
|---|---|---|---|---|---|---|
| | Change in AD patients | Change in PD patients | Reference | Change in AD patients | Change in PD patients | Reference |
| CSF | increased | increased | [20] | controversial | increased | [20,21] |
| Blood | increased | decreased | [22,23] | controversial | – | [21] |
| Brain (SN) | decreased | decreased | [24–27] | – | increased | [24] |
| Brain (HP) | decreased | decreased | [27] | increased | decreased | [27,28] |
| Brain (CB) | decreased | – | [27] | decreased | – | [27] |
| Senile plaques | enriched | – | [29] | enriched | – | [29] |

Note: AD, Alzheimer's disease dementia; PD, Parkinson's disease dementia; CSF, cerebrospinal fluid; SN, substantia nigra; HP, hippocampus; CB, cerebellum. '-', no data.

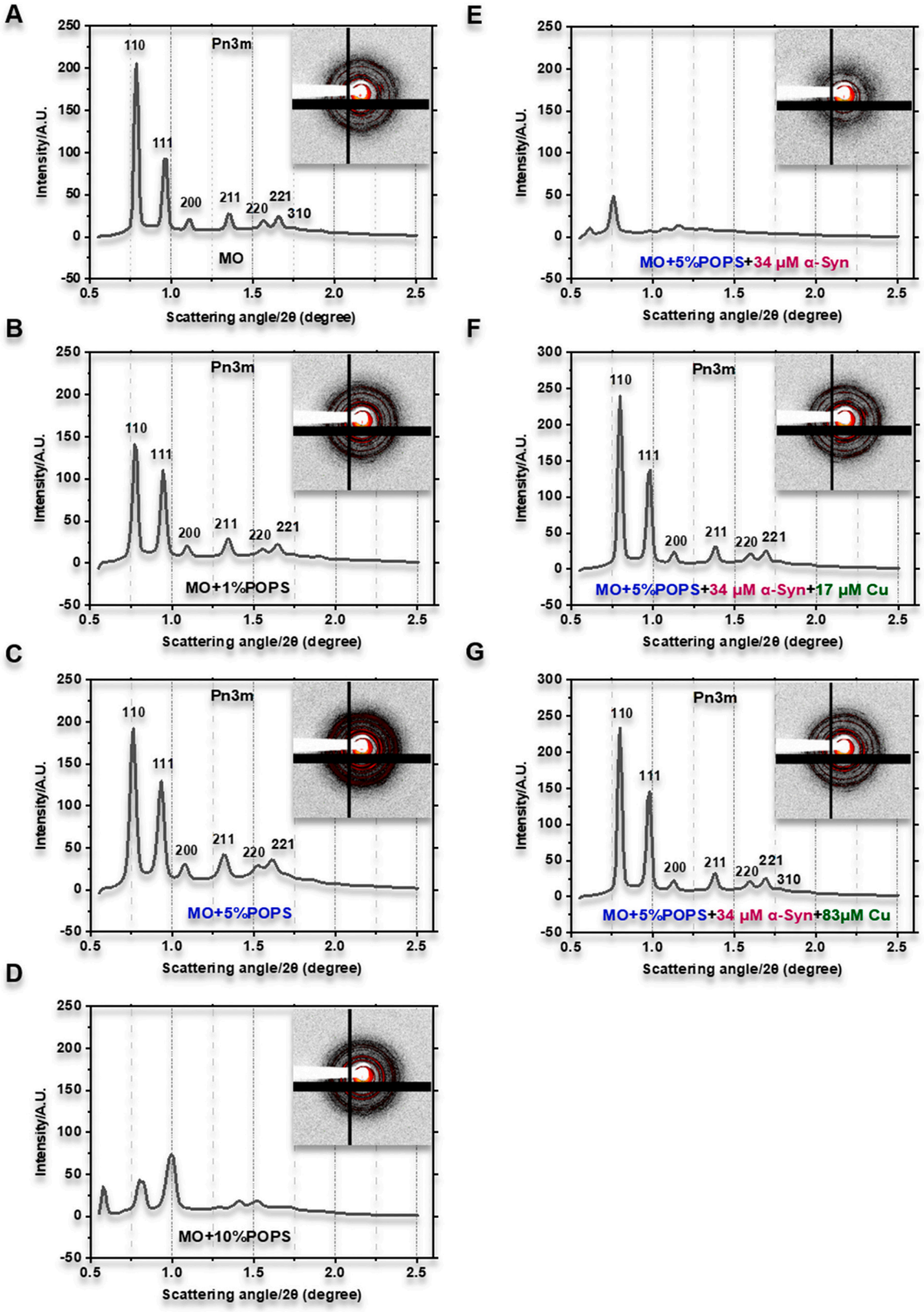


**Fig. 2.** Effect of α-Syn and $Cu^{2+}$ ions on the mesoscopic structure of lipidic cubic phase (LCP) matrix. SAXS experiments were conducted to investigate (A-D) the effect of POPS lipids on the phase behavior of monoolein (MO) lipidic cubic phase, and (E) the influence of 34 μM α-Syn on LCP made of MO supplemented with 5% POPS, as well as (F-G) the presence of 17 or 83 μM $Cu^{2+}$ ions in LCP made of MO supplemented with 5% POPS. The data indicate that α-Syn proteins destroy the Pn3m of LCP and suggest that $Cu^{2+}$ ions at used concentrations can eliminate the effect of α-Syn on the phase behavior of LCP and remain LCP as the Pn3m phase.

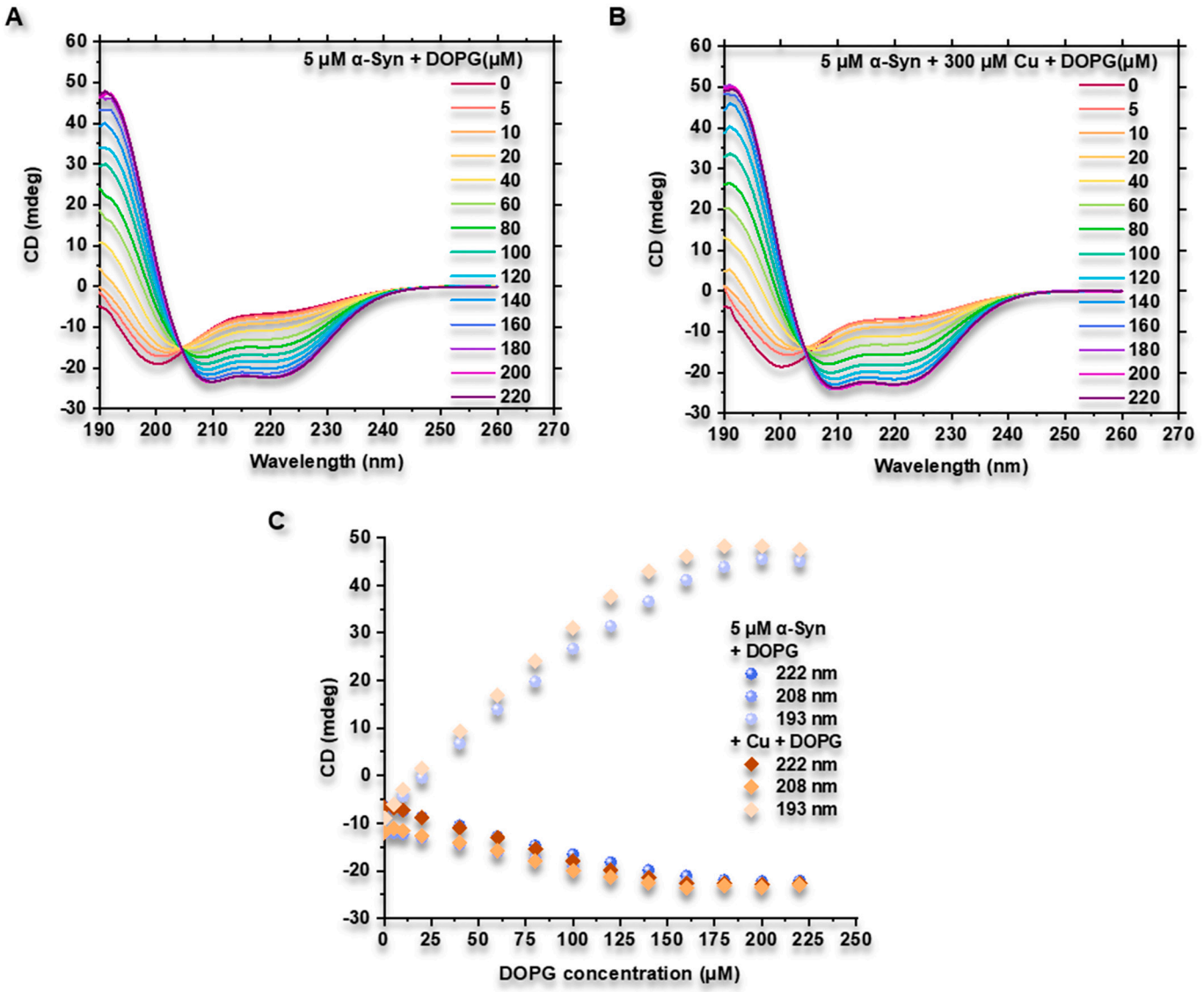


**Fig. 3.** Synergistic effect of $Cu^{2+}$ ions and DOPG liposomes on the secondary structure of α-Syn. CD experiments were conducted by gradually titrating DOPG liposomes (at concentrations of 0, 5, 10, 20, 40, 60, 80, 100, 120, 140, 160, 180, 200, 220 μM) onto 5 μM α-Syn in the absence or presence 300 μM of $Cu^{2+}$ ions. The measurements were performed immediately after the addition of the liposomes and $Cu^{2+}$ ions. (A) CD experiments in the absence of $Cu^{2+}$ ions indicate that lipid membranes induce a transition of α-Syn from random coil structure to α-helical structure. (B) In the presence of $Cu^{2+}$ ions, DOPG converted α-Syn from random coil structure into α-helical secondary structures but with a slightly stronger signal intensity of α-helical secondary structures. (C) CD signal intensities at 222 nm, 208 nm, and 193 nm of 5 μM α-Syn in the presence of DOPG liposomes with or without 300 μM $Cu^{2+}$ ions, derived from the spectra in (A) and (B).

and the states and functions of α-Syn, as well as in the normal activities of various enzymes [8], with decreased levels in the brains (SN) of PD patients [25]. Therefore, investigating how $Cu^{2+}$ ions modulate the intercommunication between α-Syn and lipid membranes will provide us with further insights into the molecular pathogenesis.

Here, we report that α-Syn proteins destabilized the Pn3m phase of LCP (Fig. 2E) and $Cu^{2+}$ ions counteracted this effect (Fig. 2F-G). $Cu^{2+}$ ions slightly enhanced the secondary structure transition of α-Syn proteins from the lipid/$Cu^{2+}$ ratio of 1:3 (Fig. 3). α-Syn proteins underwent structure changes upon possibly interacting with lipid membranes of *E. coli* cells, as we observed the chemical shift differences in Fig. 4A, and $Cu^{2+}$ interacted with α-Syn both in buffer or *E.coli* cells by interfering with its N- and C-terminus, despite that a more pronounced C-terminal interaction effect in *E.coli* cells was observed compared to the buffer solution (Fig. 4).

The effect of α-Syn proteins on the mesoscopic structure of LCP (Fig. 2E) is in agreement with the detrimental effects of α-Syn on lipid membranes [44]. It is supported by CD spectroscopy showing that DOPG liposomes induced the secondary structure transition of α-Syn from random coil to α-helix (Fig. 3A). This transition may lead to the formation of partially folded intermediates, opening the NAC domain for oligomerization [1] and resulting in the destruction of lipid membranes (Fig. 2E). The recovery of the Pn3m phase within LCP with α-Syn by the addition of $Cu^{2+}$ ions (Fig. 2F-G), could be explained by the competition binding between $Cu^{2+}$ ions and lipid membranes to monomeric α-Syn. There is an equilibrium of α-Syn proteins between cytosolic and membrane-bound states *in vivo* [45,46]. $Cu^{2+}$ ions possess two binding sites with a strong affinity that locate within the N-terminus (coordinated around M1 and/or H50) and one with low affinity sitting in the C-terminus (coordinated around D121) [8,17,36]. The binding of $Cu^{2+}$ ions onto any of the three metal binding sites located in the α-Syn protein may lead to the formation of oligomers. As a result, the binding of α-Syn monomers to the lipid membranes presumably decreases and the protein damage to the lipid membranes may be diminished (Fig. 2F-G).

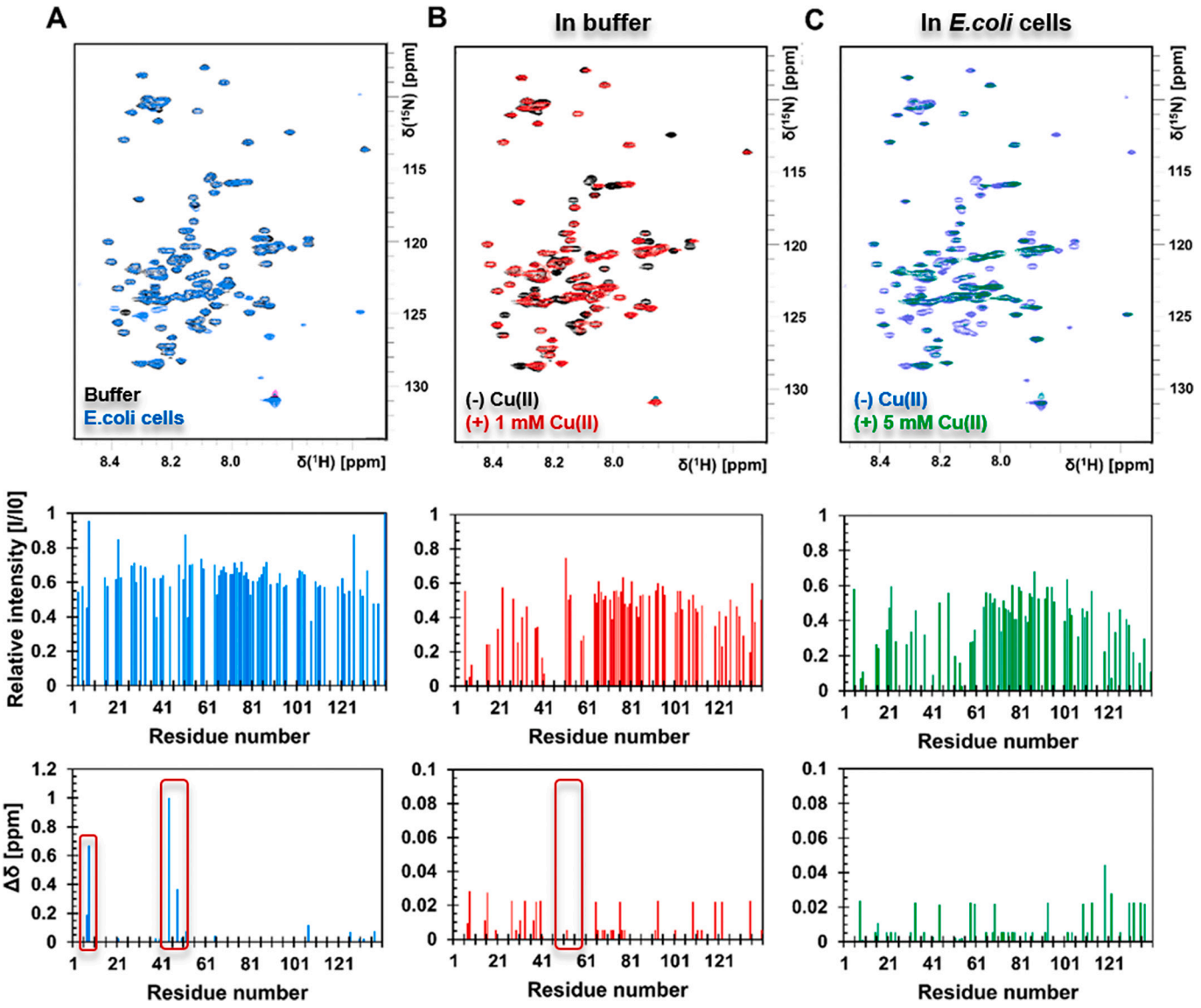


**Fig. 4.** 2D NMR $^{1}H$–$^{15}N$-HSQC spectra of $^{15}N$-α-Syn in buffer and in *E.coli* cells in the absence and presence of $Cu^{2+}$ ions. $^{1}H$–$^{15}N$-HSQC spectra comparison of (A) $^{15}N$-α-Syn in *E.coli* cells (blue spectrum) to 100 μM $^{15}N$-α-Syn in 20 mM potassium phosphate buffer pH 7.4 with 150 mM NaCl (black spectrum). In (B) are 100 μM $^{15}N$-α-Syn in 20 mM potassium phosphate buffer pH 7.4 with 150 mM NaCl in the absence of $Cu^{2+}$ (black spectrum) compared to in the presence of 1 mM $Cu^{2+}$ ions (red spectrum). (C) An estimated concentration of 60 μM $^{15}N$-α-Syn in *E.coli* cells in the absence (blue spectrum) and in the presence of 5 mM $Cu^{2+}$ ions (green spectrum). The relative amide cross-peak signal intensities are presented below the spectra. The chemical shift changes (Δδ) are presented below the relative intensities.

Also, the lipid-bound α-Syn monomers can convert into an extended α-helical structure in the presence of $Cu^{2+}$ ions, leading to a slight increase of the α-helical intensity of α-Syn from CD spectra (Fig. 3B). After the addition of $Cu^{2+}$ ions, the α-helical signal change of α-Syn in the presence of lipid vesicles is not very obvious compared to the Pn3m phase within the LCP matrix. The discrepancies in observations of two studies could be explained by the usage of two different lipid membrane systems. LCP can provide the extremely amphiphilic, air-tight and brain-mimicking condition and enable a more suitable system to detect the interaction among $Cu^{2+}$, lipid and α-Syn. On the contrary, the lipid vesicle system gives less sensitivity to the synergistic effect of $Cu^{2+}$ and lipid on α-Syn.

The schematic model of how $Cu^{2+}$ ions modulate the communication between α-Syn and lipid membranes is summarized in Fig. 5. Our observation supports other protein systems such as the one where the presence of $Cu^{2+}$ ions compromises the effect of amyloid $\beta_{42}$ on the lipid bilayers [47]. α-Syn proteins coordinate $Cu^{2+}$ ions both in its free state in a buffer as well as bound to lipid membranes [48]. The more noticeable effect in *E.coli* cells, and hence in possible contact with biological membranes, may be explained by a more stabilized metal site on the C-terminus due to the proximity and simultaneous interaction with a membrane. It has been reported that the histidine residue (H50) in α-Syn located in a membrane is shielded from metal ion interactions, with the result of a more pronounced N-terminal interaction [36], and in this case, in living *E.coli* cells the C-terminal might be compensating for the potential loss of H50 coordinating metal activity. On the other hand, the membrane-bound α-Syn population of the sample might be in equilibrium (or co-existing) with "free" α-Syn in the periplasm. Although the binding affinity of $Zn^{2+}$ ions to α-Syn is not very strong, we also observed a very similar effect of $Zn^{2+}$ ions in our SAXS studies as $Cu^{2+}$ ions. This may be caused by the $Zn^{2+}$ mediated acceleration of α-Syn fibrillation [18]. The aggregation effect of $Zn^{2+}$ ions might compromise the low binding of $Zn^{2+}$ to α-Syn.

In this study, we mimicked the air-tight and amphiphilic brain

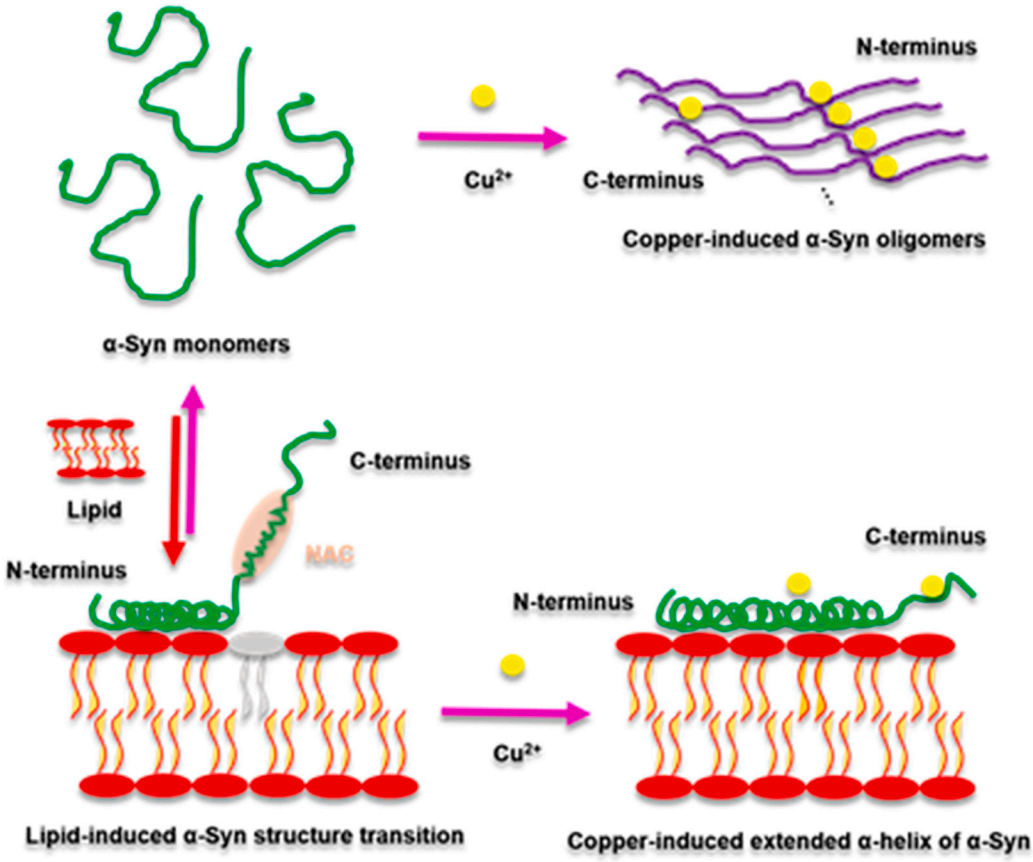


**Fig. 5.** Illustration of how $Cu^{2+}$ ions modulate the communication between α-Syn and lipid membranes. The presence of lipids induces the secondary structure transition of α-Syn from random coil to α-helix, leading to the oligomer formation directly on the surface of lipid membranes causing subsequent damage to lipid membranes (shown as lipid in light grey). Free α-Syn monomers coexist with membrane-bound forms. $Cu^{2+}$ ions may interact with α-Syn monomers more noticeably in the N-terminus in the absence of lipid membranes in buffer, leading to the oligomer formation in aqueous solution, followed by a decrease of oligomer formation on the lipid membranes. In addition, the membrane-bound form of α-Syn may adopt an extended α-helical structure and $Cu^{2+}$ may in this conformation interact with membrane-bound α-Syn within the C-terminus to a higher extent compared to in an aqueous solution.

environment by using lipidic cubic phase, and periplasm (inner and outer) membranes of *E.coli*. In these conditions, we were able to observe an interaction between lipid membranes and α-Syn in the presence of $Cu^{2+}$ ions, in comparison to lipid vesicles. As the $Cu^{2+}$ ions concentration in periplasm can not be easily estimated, the periplasm (inner and outer) membranes system in *E.coli* may not allow quantitative studies for the $Cu^{2+}$ and lipid effect on α-Syn. These lipid systems have different curvatures and amphiphilic environments, which may lead to varied sensitivity. α-Syn proteins can interfere with the structures and/or functions of membrane-containing organelles including mitochondria, by interacting with lipid membranes and components of these organelles, leading to dysfunction or even death of cells [44]. Considering the decreased levels of $Cu^{2+}$ ions in the SNs of PD patients [24,25], we found that the protective role of $Cu^{2+}$ on lipid membranes against α-Syn in LCP can provide further insight into our perception of the interplay between α-Syn, lipid membranes, and $Cu^{2+}$ ions on the molecular pathogenesis of PD.

### 3.1. Experimental procedures

#### 3.1.1. α-Syn expression and purification

Wild type α-Syn expression was conducted in phage-resistant *E.coli* BL21(DE3) cells grown on LB-Agar supplemented with 100 μg/mL Ampicillin. After overnight incubation at 37 °C and 180 rpm shaking, a single colony was transferred to a flask of 100 ml LB medium containing 100 μg/mL Ampicillin. After culture in an extended scale, isopropyl β-d-thiogalactopyranoside (IPTG) (1.0 mM) was added into the cell culture when the $OD_{600}$ reached 1.04. After incubation for 4 h at 37 °C and 180 rpm shaking, the cells were harvested by spinning down the cell culture for 20 min at 5000 rpm at 4 °C. The protein purification was performed following previously published protocols with modifications [16,49]. Briefly, after an osmotic shock, the periplasm proteins were collected and dialyzed against buffer A (20 mM Tris-HCl, pH 8.0) overnight followed by Ion Exchange Chromatography (IEX) on a HiTrap Q-Sepharose Fast Flow column (GE Healthcare) and eluted with a 0-0.5 M NaCl gradient in buffer A. Fractions containing a large amount of α-Syn were collected and α-Syn was precipitated by adding the saturated ammonium sulfate solution (~4.3 M at room temperature) stepwise to 50% saturation (1:1). The precipitated α-Syn was dissolved in 3.5 ml of 20 mM Tris-HCl, pH 7.2 and subjected to size exclusion chromatography (SEC) on a GF Hiload Superdex 75 16/600 column (GE Healthcare), and eluted with 20 mM Tris-HCl, pH 7.2 as a running buffer. The fractions were checked by SDS-PAGE, and the fractions containing α-Syn were combined and stored at -80 °C.

### 3.2. Sample preparation

#### 3.2.1. Lipid preparation

1-palmitoyl-2-oleoyl-sn-glycero-3-phospho-L-serine sodium salt (POPS, 783.99 g/mol) and monoolein (MO, 356,54 g/mol) were purchased from Sigma–Aldrich (St. Louis, MO, USA). POPS was dissolved in chloroform to a concentration of 100 mg/ml. Lipids used in sample preparation including MO, MO:POPS (99:1, 1% molar ratio), MO:POPS (95:5, 5% molar ratio), and MO:POPS (90:10, 10% molar ratio) were dried completely with nitrogen gas before usage.

#### 3.2.2. Metal solution preparation

$CuCl_2$ and $ZnCl_2$ solutions were prepared by dissolving the $CuCl_2$ and $ZnCl_2$ powder into 20 mM Tris-HCl buffer, pH 7.2, to final concentrations of 25 μM and 125 μM, mixed completely and stored at 4 °C.

#### 3.2.3. Preparation of Small-Angle X-ray Synchrotron (SAXS) samples

The samples in this study include: 1) MO, MO + 1% POPS (*w*/w), MO + 5% POPS, and MO + 10% POPS; 2) MO + 5% POPS +34 μM

α-Syn; 3) MO + 5% POPS +34 μM α-Syn + Metal ions ($CuCl_2$ and $ZnCl_2$, 17 μM and 83 μM), mixed with 4 μl of control buffer (20 mM Tris-HCl, pH 7.2). The lipidic cubic phases were prepared by referring to the published method [50]. Briefly, molten (42 °C for about 20 min) lipids including MO and MO + POPS were loaded into a pre-warmed 50 μL Hamilton gas-tight syringe with a removable needle and Teflon ferrule (Hamilton, cat. no. 81030), and the buffers (20 mM Tris-HCl, pH 7.2, alone or α-Syn) were loaded into another one and the two syringes were tightly connected with a coupler, and then the lipids: (protein-laden) buffers (3:2, volume ratio) were mixed with this coupled-syringe mixing device [51] gently until the mixture became transparent. The samples for diffraction were prepared by taking advantage of the in *meso* in situ serial crystallography (IMISX) [52]. The prepared lipidic cubic phases were then dispersed manually into the wells of the plate at 20 °C followed by the addition of 4 μL of 20 mM Tris-HCl buffer, pH 7.2, with or without metal ions. The wells were then sealed by overlaying the Mylar film stuck on the glass cover plate and rolling gently the double-sandwich plate with a brayer, in this way, the plate was housed in the glass plate. The samples were prepared about 5 h before the diffraction and left at room temperature.

### 3.3. SAXS data collection

Immediately before the diffraction, the plate was separated from the glass bases, cut into sections (1*4 wells) and bonded onto the sample holder with the double-stick stape. Diffraction data collection was performed by referring to the published method [52] at room temperature (20 °C) with 10*20 $\mu m^2$ X-ray beam size at 12.4 keV (1.0332 Å) on beamline PXII (X10SA, the Swiss Light Source, Villigen, Switzerland). The diffraction was carried out using an EIGER2 16 M detector with a sample-to-detector distance of 1200 mm and a sample-to-beamstop distance of 80 mm. Data corresponding to 2*50 grids was collected with a beam transmission of 100% and an exposure time of 0.2 s. In addition, as controls, the Mylar film alone and Mylar film+buffer were diffracted as well.

The control samples including MO and MO supplemented with $Cu^{2+}$ ions were prepared with cyclic olefin copolymer (COC) film, aiming to check the influence of $Cu^{2+}$ ions on the phase behavior of LCP. The data collection of control samples was performed at beamline PXI (X06SA, the Swiss Light Source, Villigen, Switzerland), and the results are shown in Fig.S1.

### 3.4. SAXS data analysis

The data were analyzed with the Albula software (DECTRIS, Switzerland) and then exported and saved as an Excel file, obtaining the intensity (I) vs scattering angle (2θ), with around 15 repeats for each sample. The obtained intensities of each sample were averaged and the average background value was subtracted from each average intensity. The scattering angles were converted into radians. The d spaces and resolutions (q) of each sample were then calculated by using the Bragg's law

$$2d\sin\theta = n\lambda$$

where d = interplanar distance, θ = scattering angle, n = positive integer, λ = wavelength of the incident wave. The intensity vs scattering angle was plotted with the software Origin (Version 2018, OriginLab, USA).

### 3.5. Liposome preparation

10 mg/mL DOPG (1,2-Dioleoyl-sn-glycero-3-phospho-rac-(1-glycerol)) was dried with Argon gas, followed by vacuum drying overnight. The dried DOPG was sonicated and then dissolved in 25 mM potassium phosphate buffer, pH 7.4, obtaining DOPG liposomes at a concentration of 10 mg/mL.

### 3.6. Circular dichroism (CD) spectroscopy

For the CD spectroscopy measurements, the samples were prepared by titrating metal ions into 5 μM α-Syn to final concentrations of 0, 5, 25, 75, 150, and 300 μM and by titrating DOPG liposomes onto 5 μM α-Syn with or without 300 μM metal ions ($Cu^{2+}$ and $Zn^{2+}$) in 25 mM potassium phosphate buffer, pH 7.4. The CD spectra were recorded in the far-UV region from 190 to 260 nm with a Chirascan plus CD spectrometer (Applied Photophysics Limited, U.K.). The samples were measured in a quartz cuvette with a path length of 10 mm at 37 °C immediately after stirring using a pipette, with a step size of 1.0 nm, a bandwidth of 1.0 nm, and a time per point of 0.5 s. The spectra were recorded immediately after the preparation of 5 μM α-Syn solution, the addition of metal ions, and the titration of DOPG liposomes (final concentrations of 0, 5, 10, 20, 40, 60, 80, 100, 120, 140, 160, 180, 200, and 220 μM). The curves were smoothed with a function of 10 points and replotted with the software Origin (Version 2018, OriginLab, USA).

### 3.7. In-cell nuclear magnetic resonance (NMR)

In-cell NMR measurements of α-Syn proteins were prepared as described previously [53]. A single colony (*E. coli* (BL21 (DE3) pLysS cells) with the α-Syn plasmid was cultured overnight in 15 ml LB medium. The overnight supernatant was discarded after the centrifugation at 3000 rpm for 15 min and the cell pellet was resuspended and grown in 250 ml M9 minimal medium [54] containing 100 μg/ml of $^{15}NH_4Cl$ (Sigma) in a shaker at 180 rpm, 37 °C. Until $OD_{600}$ reached 0.8, cell cultures were induced with 1 mM IPTG for 4 h and then centrifuged for 20 min at 4 °C, 3000 rpm. The pellet was resuspended by 1.5 ml supernatant for the *in-cell* NMR measurement. A sample of the resuspended cells: $^2H_2O$ at 90:10 (*v*/v ratio) was prepared to acquire the *in-cell* spectrum. The concentration of $^{15}N$-labelled α-Syn was estimated by comparison to a known $^{15}N$-labelled α-Syn concentration by comparing the amide signal intensities in $^1H$–$^{15}N$-HSQC spectra. $^1H$–$^{15}N$-HSQC spectra were recorded on a 700 MHz NMR spectrometer (Bruker AVIII 700) equipped with a cryogenic probe 1H/13C/15 N TCI cryoprobe (AV700). The spectra were recorded at 6 °C. The assignment used for the $^1H$–$^{15}N$-HSQC spectra has been published previously by other groups [55]. The software Topspin v.4.0.7 was used to analyze the data.

## CRediT authorship contribution statement

**Hongzhi Wang:** Investigation, Methodology, Writing - original draft. **Cecilia Mörman:** Data curation, Validation, Formal analysis, Writing - review & editing. **Rebecca Sternke-Hoffmann:** Validation. **Chia-Ying Huang:** Investigation, Validation, Methodology. **Andrea Prota:** Investigation. **Pikyee Ma**: Methodology, Data curation. **Jinghui Luo:** Conceptualization, Investigation, Supervision, Funding acquisition, Project administration, Resources, Writing - review & editing.

## Declaration of Competing Interest

None

## Data availability

Data will be made available on request.

## Acknowledgements

We acknowledge financial support from the Swedish research council (2021-00418, C. M.) and the Swiss national scientific foundation (310030_197626, J. L.), the Brightfocus foundation (A20201759S, J. L.) and the PSI research grant (J. L.).

## Appendix A. Supplementary data

Supplementary data to this article can be found online at https://doi.org/10.1016/j.jinorgbio.2022.111945.

## References


[1] M. Kiechle, V. Grozdanov, K.M. Danzer, The role of lipids in the initiation of alpha-Synuclein Misfolding, Front Cell Dev Biol 8 (2020), 562241.
[2] G. Fusco, A. De Simone, T. Gopinath, V. Vostrikov, M. Vendruscolo, C.M. Dobson, G. Veglia, Direct observation of the three regions in alpha-synuclein that determine its membrane-bound behaviour, Nat. Commun. 5 (2014) 3827.
[3] C. Masaracchia, M. Hnida, E. Gerhardt, T. Lopes da Fonseca, A. Villar-Pique, T. Branco, M.A. Stahlberg, C. Dean, C.O. Fernandez, I. Milosevic, T.F. Outeiro, Membrane binding, internalization, and sorting of alpha-synuclein in the cell, Acta Neuropathol Commun 6 (2018) 79.
[4] J. Varkey, J.M. Isas, N. Mizuno, M.B. Jensen, V.K. Bhatia, C.C. Jao, J. Petrlova, J. C. Voss, D.G. Stamou, A.C. Steven, R. Langen, Membrane curvature induction and tubulation are common features of synucleins and apolipoproteins, J. Biol. Chem. 285 (2010) 32486–32493.
[5] M.M. Ouberai, J. Wang, M.J. Swann, C. Galvagnion, T. Guilliams, C.M. Dobson, M. E. Welland, Alpha-Synuclein senses lipid packing defects and induces lateral expansion of lipids leading to membrane remodeling, J. Biol. Chem. 288 (2013) 20883–20895.
[6] M. Pantusa, B. Vad, O. Lillelund, L. Kjaer, D. Otzen, R. Bartucci, Alpha-synuclein and familial variants affect the chain order and the thermotropic phase behavior of anionic lipid vesicles, Biochim. Biophys. Acta 1864 (2016) 1206–1214.
[7] C. Galvagnion, The role of lipids interacting with alpha-Synuclein in the pathogenesis of Parkinson's disease, J. Parkinsons Dis. 7 (2017) 433–450.
[8] E. Carboni, P. Lingor, Insights on the interaction of alpha-synuclein and metals in the pathophysiology of Parkinson's disease, Metallomics : integrated biometal science 7 (2015) 395–404.
[9] G. Gromadzka, B. Tarnacka, A. Flaga, A. Adamczyk, Copper Dyshomeostasis in neurodegenerative diseases-therapeutic implications, Int. J. Mol. Sci. 21 (2020).
[10] A.I. Bush, Metals and neuroscience, Curr. Opin. Chem. Biol. 4 (2000) 184–191.
[11] E.M. Landau, J.P. Rosenbusch, Lipidic cubic phases: a novel concept for the crystallization of membrane proteins, Proc. Natl. Acad. Sci. U. S. A. 93 (1996) 14532–14535.
[12] M. Caffrey, A comprehensive review of the lipid cubic phase or in meso method for crystallizing membrane and soluble proteins and complexes, Acta Crystallogr F Struct Biol Commun 71 (2015) 3–18.
[13] H. Qiu, M. Caffrey, The phase diagram of the monoolein/water system: metastability and equilibrium aspects, Biomaterials 21 (2000) 223–234.
[14] E.R. Middleton, E. Rhoades, Effects of curvature and composition on alpha-synuclein binding to lipid vesicles, Biophys. J. 99 (2010) 2279–2288.
[15] I.M. Pranke, V. Morello, J. Bigay, K. Gibson, J.M. Verbavatz, B. Antonny, C. L. Jackson, Alpha-Synuclein and ALPS motifs are membrane curvature sensors whose contrasting chemistry mediates selective vesicle binding, J. Cell Biol. 194 (2011) 89–103.
[16] C. Huang, G. Ren, H. Zhou, C.C. Wang, A new method for purification of recombinant human alpha-synuclein in Escherichia coli, Protein Expr. Purif. 42 (2005) 173–177.
[17] R.M. Rasia, C.W. Bertoncini, D. Marsh, W. Hoyer, D. Cherny, M. Zweckstetter, C. Griesinger, T.M. Jovin, C.O. Fernandez, Structural characterization of copper(II) binding to alpha-synuclein: insights into the bioinorganic chemistry of Parkinson's disease, Proc. Natl. Acad. Sci. U. S. A. 102 (2005) 4294–4299.
[18] A.A. Valiente-Gabioud, V. Torres-Monserrat, L. Molina-Rubino, A. Binolfi, C. Griesinger, C.O. Fernandez, Structural basis behind the interaction of Zn(2)(+) with the protein alpha-synuclein and the Abeta peptide: a comparative analysis, J. Inorg. Biochem. 117 (2012) 334–341.
[19] N. Gonzalez, T. Arcos-Lopez, A. Konig, L. Quintanar, M. Menacho Marquez, T. F. Outeiro, C.O. Fernandez, Effects of alpha-synuclein post-translational modifications on metal binding, J. Neurochem. 150 (2019) 507–521.
[20] I. Hozumi, T. Hasegawa, A. Honda, K. Ozawa, Y. Hayashi, K. Hashimoto, M. Yamada, A. Koumura, T. Sakurai, A. Kimura, Y. Tanaka, M. Satoh, T. Inuzuka, Patterns of levels of biological metals in CSF differ among neurodegenerative diseases, J. Neurol. Sci. 303 (2011) 95–99.
[21] S. Ayton, D.I. Finkelstein, R.A. Cherny, A.I. Bush, P.A. Adlard, Zinc in Alzheimer's and Parkinson's diseases, in: R.H. Kretsinger, V.N. Uversky, E.A. Permyakov (Eds.), Encyclopedia of Metalloproteins, Springer New York, New York, NY, 2013, pp. 2433–2441.
[22] R. Squitti, I. Simonelli, M. Ventriglia, M. Siotto, P. Pasqualetti, A. Rembach, J. Doecke, A.I. Bush, Meta-analysis of serum non-ceruloplasmin copper in Alzheimer's disease, J. Alzheimers Dis. 38 (2014) 809–822.
[23] E.Y. Ilyechova, I.V. Miliukhina, I.A. Orlov, Z.M. Muruzheva, L.V. Puchkova, M. N. Karpenko, A low blood copper concentration is a co-morbidity burden factor in Parkinson's disease development, Neurosci. Res. 135 (2018) 54–62.
[24] D.T. Dexter, F.R. Wells, A.J. Lees, F. Agid, Y. Agid, P. Jenner, C.D. Marsden, Increased nigral iron content and alterations in other metal ions occurring in brain in Parkinson's disease, J. Neurochem. 52 (1989) 1830–1836.
[25] K.M. Davies, S. Bohic, A. Carmona, R. Ortega, V. Cottam, D.J. Hare, J.P. Finberg, S. Reyes, G.M. Halliday, J.F. Mercer, K.L. Double, Copper pathology in vulnerable brain regions in Parkinson's disease, Neurobiol. Aging 35 (2014) 858–866.
[26] S. Genoud, B.R. Roberts, A.P. Gunn, G.M. Halliday, S.J.G. Lewis, H.J. Ball, D. J. Hare, K.L. Double, Subcellular compartmentalisation of copper, iron, manganese, and zinc in the Parkinson's disease brain, Metallomics 9 (2017) 1447–1455.
[27] M. Scholefield, S.J. Church, J. Xu, S. Patassini, F. Roncaroli, N.M. Hooper, R. D. Unwin, G.J.S. Cooper, Widespread decreases in cerebral copper are common to Parkinson's disease dementia and Alzheimer's disease dementia, Front. Aging Neurosci. 13 (2021), 641222.
[28] P.A. Adlard, A.I. Bush, Metals and Alzheimer's disease, J. Alzheimers Dis. 10 (2006) 145–163.
[29] M.A. Lovell, J.D. Robertson, W.J. Teesdale, J.L. Campbell, W.R. Markesbery, Copper, iron and zinc in Alzheimer's disease senile plaques, J. Neurol. Sci. 158 (1998) 47–52.
[30] V. Cherezov, J. Clogston, Y. Misquitta, W. Abdel-Gawad, M. Caffrey, Membrane protein crystallization in meso: lipid type-tailoring of the cubic phase, Biophys. J. 83 (2002) 3393–3407.
[31] H.Y. Kim, B.X. Huang, A.A. Spector, Phosphatidylserine in the brain: metabolism and function, Prog. Lipid Res. 56 (2014) 1–18.
[32] S. Takamori, M. Holt, K. Stenius, E.A. Lemke, M. Gronborg, D. Riedel, H. Urlaub, S. Schenck, B. Brugger, P. Ringler, S.A. Muller, B. Rammner, F. Grater, J.S. Hub, B. L. De Groot, G. Mieskes, Y. Moriyama, J. Klingauf, H. Grubmuller, J. Heuser, F. Wieland, R. Jahn, Molecular anatomy of a trafficking organelle, Cell 127 (2006) 831–846.
[33] H. Xicoy, B. Wieringa, G.J.M. Martens, The role of lipids in Parkinson's disease, Cells 8 (2019).
[34] M. Stockl, P. Fischer, E. Wanker, A. Herrmann, Alpha-synuclein selectively binds to anionic phospholipids embedded in liquid-disordered domains, J. Mol. Biol. 375 (2008) 1394–1404.
[35] C.G. Dudzik, E.D. Walter, B.S. Abrams, M.S. Jurica, G.L. Millhauser, Coordination of copper to the membrane-bound form of alpha-synuclein, Biochemistry 52 (2013) 53–60.
[36] D. Valensin, S. Dell'Acqua, H. Kozlowski, L. Casella, Coordination and redox properties of copper interaction with alpha-synuclein, J. Inorg. Biochem. 163 (2016) 292–300.
[37] A. Binolfi, G.R. Lamberto, R. Duran, L. Quintanar, C.W. Bertoncini, J.M. Souza, C. Cervenansky, M. Zweckstetter, C. Griesinger, C.O. Fernandez, Site-specific interactions of cu(II) with alpha and beta-synuclein: bridging the molecular gap between metal binding and aggregation, J. Am. Chem. Soc. 130 (2008) 11801–11812.
[38] C. Rensing, G. Grass, Escherichia coli mechanisms of copper homeostasis in a changing environment, FEMS Microbiol. Rev. 27 (2003) 197–213.
[39] J.-I. Ishihara, T. Mekubo, C. Kusaka, S. Kondo, H. Aiba, S. Ishikawa, N. Ogasawara, T. Oshima, H. Takahashi, Critical role of the periplasm in copper homeostasis in Gram-negative bacteria, bioRxiv (2020), https://doi.org/10.1101/2020.08.17.251918.
[40] C.J. Kershaw, N.L. Brown, C. Constantinidou, M.D. Patel, J.L. Hobman, The expression profile of Escherichia coli K-12 in response to minimal, optimal and excess copper concentrations, Microbiology 151 (2005) 1187–1198.
[41] M.M. Dedmon, K. Lindorff-Larsen, J. Christodoulou, M. Vendruscolo, C.M. Dobson, Mapping long-range interactions in alpha-synuclein using spin-label NMR and ensemble molecular dynamics simulations, J. Am. Chem. Soc. 127 (2005) 476–477.
[42] C.A. Waudby, C. Camilloni, A.W. Fitzpatrick, L.D. Cabrita, C.M. Dobson, M. Vendruscolo, J. Christodoulou, In-cell NMR characterization of the secondary structure populations of a disordered conformation of alpha-synuclein within E. coli cells, PLoS One 8 (2013), e72286.
[43] Y. Li, C. Zhao, F. Luo, Z. Liu, X. Gui, Z. Luo, X. Zhang, D. Li, C. Liu, X. Li, Amyloid fibril structure of alpha-synuclein determined by cryo-electron microscopy, Cell Res. 28 (2018) 897–903.
[44] L.D. Bernal-Conde, R. Ramos-Acevedo, M.A. Reyes-Hernandez, A.J. Balbuena-Olvera, I.D. Morales-Moreno, R. Arguero-Sanchez, B. Schule, M. Guerra-Crespo, Alpha-Synuclein physiology and pathology: a perspective on cellular structures and organelles, Front. Neurosci. 13 (2019) 1399.
[45] H.J. Lee, C. Choi, S.J. Lee, Membrane-bound alpha-synuclein has a high aggregation propensity and the ability to seed the aggregation of the cytosolic form, J. Biol. Chem. 277 (2002) 671–678.
[46] V.N. Uversky, D. Eliezer, Biophysics of Parkinson's disease: structure and aggregation of alpha-synuclein, Curr. Protein Pept. Sci. 10 (2009) 483–499.
[47] T.L. Lau, E.E. Ambroggio, D.J. Tew, R. Cappai, C.L. Masters, G.D. Fidelio, K. J. Barnham, F. Separovic, Amyloid-beta peptide disruption of lipid membranes and the effect of metal ions, J. Mol. Biol. 356 (2006) 759–770.
[48] Y.H. Sung, C. Rospigliosi, D. Eliezer, NMR mapping of copper binding sites in alpha-synuclein, Biochim. Biophys. Acta 1764 (2006) 5–12.
[49] M.M. Wordehoff, W. Hoyer, Alpha-Synuclein aggregation monitored by Thioflavin T fluorescence assay, Bio Protoc 8 (2018).
[50] P. Ma, D. Weichert, L.A. Aleksandrov, T.J. Jensen, J.R. Riordan, X. Liu, B. K. Kobilka, M. Caffrey, The cubicon method for concentrating membrane proteins in the cubic mesophase, Nat. Protoc. 12 (2017) 1745–1762.
[51] A. Cheng, B. Hummel, H. Qiu, M. Caffrey, A simple mechanical mixer for small viscous lipid-containing samples, Chem. Phys. Lipids 95 (1998) 11–21.
[52] C.Y. Huang, V. Olieric, P. Ma, N. Howe, L. Vogeley, X. Liu, R. Warshamanage, T. Weinert, E. Panepucci, B. Kobilka, K. Diederichs, M. Wang, M. Caffrey, In meso in situ serial X-ray crystallography of soluble and membrane proteins at cryogenic temperatures, Acta Crystallogr D Struct Biol 72 (2016) 93–112.

[53] B.C. McNulty, G.B. Young, G.J. Pielak, Macromolecular crowding in the Escherichia coli periplasm maintains alpha-synuclein disorder, J. Mol. Biol. 355 (2006) 893–897.
[54] Z. Serber, R. Ledwidge, S.M. Miller, V. Dotsch, Evaluation of parameters critical to observing proteins inside living Escherichia coli by in-cell NMR spectroscopy, J. Am. Chem. Soc. 123 (2001) 8895–8901.
[55] D. Eliezer, E. Kutluay, R. Bussell Jr., G. Browne, Conformational properties of alpha-synuclein in its free and lipid-associated states, J. Mol. Biol. 307 (2001) 1061–1073.